Erzincan Üniversitesi
Fen Bilimleri Enstitüsü Dergisi
2024, 17(3), 826-839
ISSN: 1307-9085, e-ISSN: 2149-4584
Araştırma Makalesi

Erzincan University
Journal of Science and Technology
2024, 17(3), 826-839
DOI: 10.18185/erzifbed.1564348
Research Article

Modeling, Analysis, and Comparison of Rectangular Waveguide Structures Having Glide Symmetrical Step Discontinuity with Periodic Dielectric Loading

Agâh Oktay ERTAY[1*]

[1]Erzincan Binali Yıldırım University, Faculty of Engineering and Architecture, Department of Electrical and Electronics Engineering, 24002, Erzincan, Türkiye

Received: 09/10/2024, **Revised:** 21/11/2024, **Accepted:** 28/11/2024, **Published:** 31/12/2024

Abstract

This paper presents an analysis of the dispersion and $|S_{21}|$ frequency characteristics of three periodic structures constructed in rectangular waveguides. Unit cells with dielectric-loaded step discontinuities based on double steps, symmetric double steps, and glide-symmetric double steps were investigated using full-wave electromagnetic simulation software. All dispersion diagram results obtained from the three different models are compared to each other by fixing the period of the unit cell ($p = 13.68mm$) for each periodic structure. $|S_{21}|$ frequency characteristics of the first propagating mode are examined for finite implementations of all considered structures. The transmission characteristics of different numbers of periodic arrangements of each periodic unit cell were investigated. Then, the effect of geometric variations, including glide symmetry, on the transmission characteristics is investigated by keeping the number of unit cells constant ($N = 10$). Furthermore, the filter performance characteristics of the proposed structure are compared with those of the reported studies in the open literature.

Keywords: dispersion analysis, glide symmetry, periodic structures, rectangular waveguides, step discontinuity

Periyodik Dielektrik Yüklü Kayma Simetrili Adım Süreksizliğine Sahip Dikdörtgen Dalga Kılavuzu Yapılarının Modellenmesi, Analizi ve Karşılaştırılması

Öz

Bu makale, dikdörtgen dalga kılavuzlarında oluşturulan üç periyodik yapının dispersiyon ve $|S_{21}|$ frekans karakteristiklerinin analizini sunmaktadır. Çift adım, simetrik çift adım ve kayma-simetrik çift adıma dayalı dielektrik yüklü adım süreksizliğine sahip birim hücreler, tam dalga elektromanyetik benzetim yazılımı kullanılarak incelenmiştir. Üç farklı modelden elde edilen tüm dispersiyon diyagramı sonuçları, her periyodik yapı için birim hücrenin periyodunu sabitleyerek ($p = 13.68mm$) birbirleriyle karşılaştırılmıştır. Tüm dikkate alınan yapıların sonlu yapıları için ilk yayılan modun $|S_{21}|$ frekans karakteristikleri incelenmiştir. Her periyodik birim hücrenin farklı sayıdaki periyodik dizilimlerinin iletim karakteristikleri incelenmiştir. Sonra, birim hücre sayısı sabit tutularak ($N = 10$) kayma simetrisi de dâhil olmak üzere geometrik değişimlerin iletim karakteristikleri üzerindeki etkisi incelenmiştir. Ayrıca, önerilen yapının filtre performans özellikleri açık literatürde rapor edilen çalışmalarla karşılaştırılmıştır.

Anahtar Kelimeler: adım süreksizliği, dikdörtgen dalga kılavuzları, dispersiyon analizi, kayma simetrisi, periyodik yapılar

*Corresponding Author: aoertay@erzincan.edu.tr
Agâh Oktay ERTAY, https://orcid.org/0000-0001-6791-0947

1. Introduction

The investigation of electromagnetic wave propagation and its effects on periodic structures is a current and interesting research area [1]. By appropriately selecting the dimensions of the geometries and medium properties in periodic structures, passband/stopband regions can be obtained. These properties are widely exploited in waveguides [2, 3], substrate-integrated waveguides [4], microstrip [5] type filters, and leaky wave antennas [6]. In recent years, the investigation of the dispersion characteristics of unit cell designs of dielectric-loaded metallic rectangular [7] and corrugated parallel-plate waveguide [8–10] periodic structures has become a popular topic. Higher-symmetry unit cell modeling of such structures is frequently preferred due to its features, which provide benefits in applications such as low dispersion, wider stopbands, and passbands [11–13].

In dielectric-loaded rectangular waveguides, step discontinuity structures are used for purposes such as examining field distribution changes [14] and obtaining passband/stopband regions [15, 16]. It is well known that the use of multiple-step discontinuities in rectangular waveguide unit cells creates deeper stopbands and passband fluctuations when the structure is connected in a finite number of cascades [15, 16]. However, to the best of our knowledge, the modeling and analysis of the unit cell structure with glide-symmetric step discontinuity in dielectric-loaded rectangular waveguides has not been investigated. To fill this gap in the literature, systematic modeling and analysis results are presented in this study. First, a unit cell with classical step discontinuity is modeled. In the second stage, a second-step discontinuity is modeled in the opposite direction to the step discontinuity region of the model used in the first stage. In the final stage, the glide symmetry approach is applied to the model created in the second stage. Dispersion diagrams of the structures are obtained, and the passband/stopband regions of periodic structures are analyzed. A finite periodic implementation is performed for all models, and frequency characteristics are examined. The details of these modellings and the results are given in the following sections.

2. Material and Methods

In this section, the dispersion properties of the selected unit cell models will be analyzed.

2.1. Considered Unit Cell Geometries for the Analysis

A periodic structure with glide symmetry is a structure that is invariant under the translation of the half-period of the structure in the periodicity direction and mirroring with respect to the glide plane [9, 10]. Accordingly, the glide operator (G) for a periodic structure with a direction period p can be written as [17]:

$$G = \begin{cases} x \rightarrow -x \\ y \rightarrow y \\ z \rightarrow z + p/2 \end{cases} \quad (1)$$

Figure 1 shows the geometries of the investigated unit cell models. From Figure 1(a) to Figure 1(c), the step-by-step application of the glide symmetry operation (G) given in equation (1) in

a rectangular waveguide with step discontinuity is given. Figure 1(a) shows the rectangular waveguide unit cell structure with conventional step discontinuity, with examples from the literature [14-16]. Figure 1(b) shows the unit cell of the rectangular waveguide geometry with a symmetric double-step discontinuity [18]. Figure 1(c) shows the newly proposed rectangular waveguide unit cell with double-step discontinuity generated by glide symmetry. All models were homogeneously loaded with the same dielectric material. To obtain the dispersion diagrams of the unit cell models, the generalized scattering matrices of these structures were obtained using the CST Microwave Studio Frequency Domain Solver based on the Finite Element Method (FEM). All waveguides consist of metallic walls with a thickness of t as indicated in Figure 2. The interior of the structure is filled with a dielectric material with $\varepsilon_r = 4.8$. The boundary conditions in x and y are assigned as electric (Et = 0) since all side walls are metallic. All unit cell structures are excited by a waveguide port operating in 10 modes from the input and output reference planes. To find the Floquet modes and stop bands supported by each unit cell, the obtained generalized scattering matrix elements are substituted into the eigenvalue equation [3]:

$$\begin{bmatrix} \boldsymbol{I} & -\boldsymbol{S_{11}} \\ \boldsymbol{0} & -\boldsymbol{S_{12}} \end{bmatrix} \begin{bmatrix} \boldsymbol{b_1} \\ \boldsymbol{a_1} \end{bmatrix} + \lambda \begin{bmatrix} -\boldsymbol{S_{12}} & \boldsymbol{0} \\ -\boldsymbol{S_{22}} & \boldsymbol{I} \end{bmatrix} \begin{bmatrix} \boldsymbol{b_1} \\ \boldsymbol{a_1} \end{bmatrix} = \boldsymbol{0} \tag{2}$$

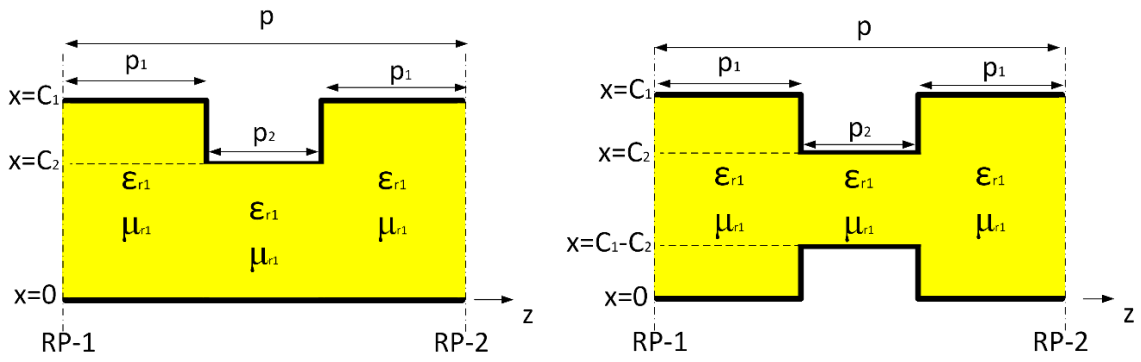

(a)

(b)

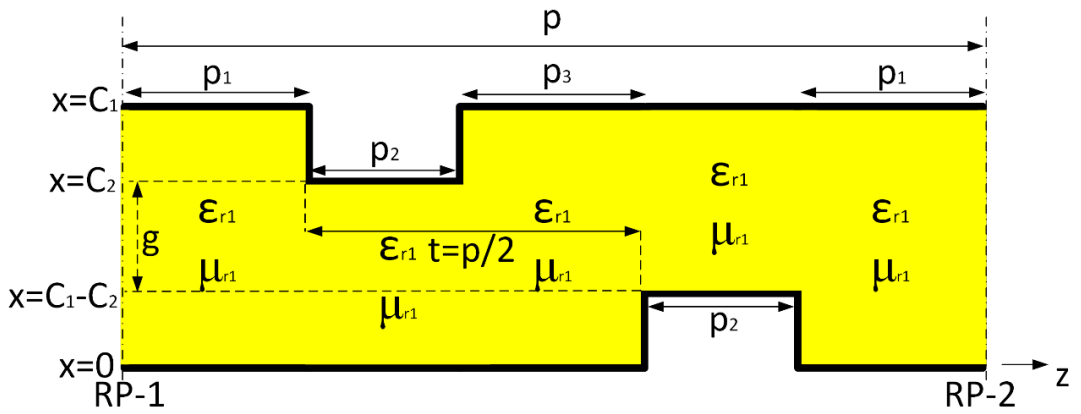

(c)

Figure 1. Unit cell of periodic rectangular waveguide with the following different geometries: (a) one step discontinuity with symmetric dielectric loading (conventional structure – 1 (CS - 1)) (b) Two symmetric step discontinuity with dielectric loading (conventional structure – 2 (CS - 2)) (c) glide symmetric step discontinuity with dielectric loading (proposed structure (PS)). p depicts the period of given unit cell geometries. μ_{r1} is taken as 1.

$\boldsymbol{I}$, ($\boldsymbol{S_{ii}}, \boldsymbol{S_{ij}}$) and ($\boldsymbol{a_1}, \boldsymbol{b_1}$) in Equation (2) denote the unit matrix, block S-matrix elements, and complex amplitudes incident and reflected from reference plane-1 (RP-1), respectively. For single Floquet mode propagation, eigenvalue λ is defined as $\lambda_{1,2} = e^{\pm j\theta}, \theta = \beta p \ \in 0, \pi$ where β is Floquet phase factor [3, 19]. With fine frequency scanning, the passband and stopband regions can be determined by finding whether there is at least one propagating mode corresponding to the eigenvalue pair at each step.

2.2. Dispersion Diagram Analysis

Figures 2-4 shows the first passband/stopband regions of dispersion diagrams of the unit cell geometries of CS-1, CS-2, and PS in Figure 1. There is a two-stage flow for obtaining these graphs. In the first stage, the investigated unit cells are simulated in CST using the simulation details given in the previous subsection. In the second stage, the dispersion diagrams of the unit cells are obtained by substituting the obtained generalized scattering matrices into Equation 2 and solving this equation. The parameters of all models are presented in Figure 1, and the values of these parameters are given in Figures 2-4. The period of each unit cell was kept constant at the same value to observe the effects of the modification of each stage and the glide symmetry on the dispersion diagrams and transmission characteristics. Despite the homogeneous dielectric loading, the step discontinuities in the cross-sections caused high-order mode interactions.

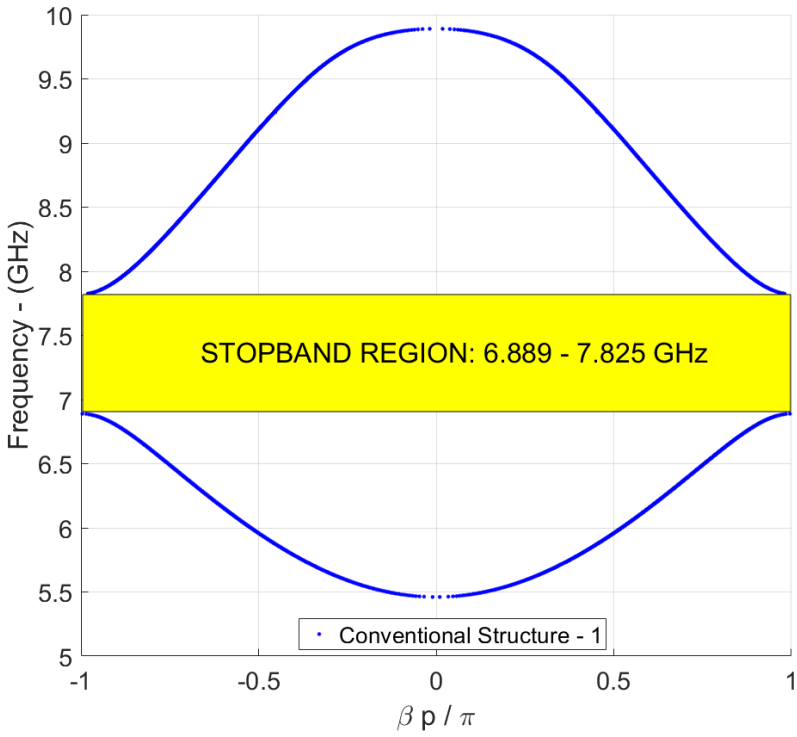

Figure 2. Dispersion diagram of conventional structure-1 given in Figure 1 (a) with the following parameters: $C_1 = 14.8$mm, $C_2 = 0.7C_1$, $p_1 = 0.416C_1$, $p_2 = 0.0925C_1$, $h = 0.5$mm, $t = 0.035$mm, $\varepsilon_{r1} = 4.8$, $p = 2p_1 + p_2 = 0.9245C_1$. t and h are the thickness and the height (in the y-direction) of the rectangular waveguide walls, respectively.

To monitor these effects on the mode of the periodic structure, 10 excitation modes are considered sufficient. The first Floquet mode of CS-1 started at approximately 5.5 GHz and

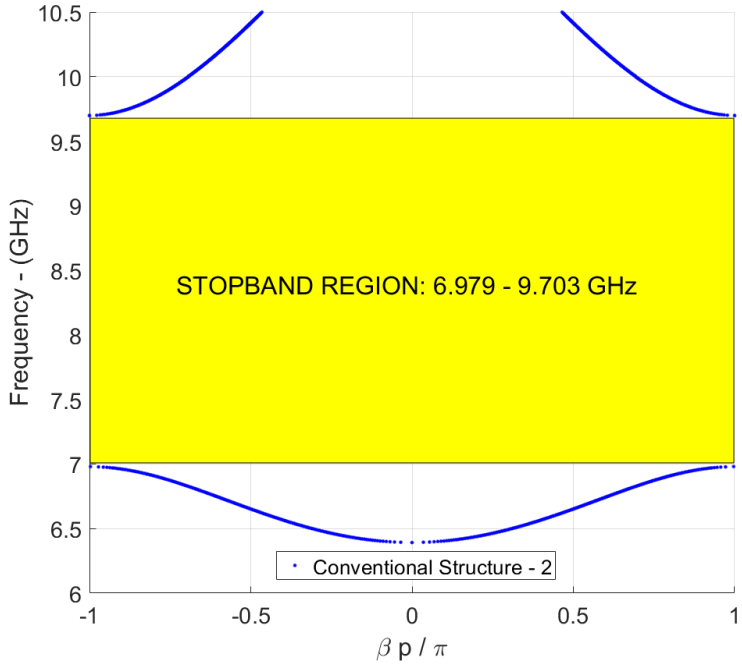

Figure 3. Dispersion diagram of conventional structure-2 given in Figure 1 (b) with the following parameters: $C_1 = 14.8$mm, $C_2 = 0.7C_1$, $p_1 = 0.416C_1$, $p_2 = 0.0925C_1$, $h = 0.5$mm, $t = 0.035$mm, $\varepsilon_{r1} = 4.8$, $p = 2p_1 + p_2 = 0.9245C_1$.

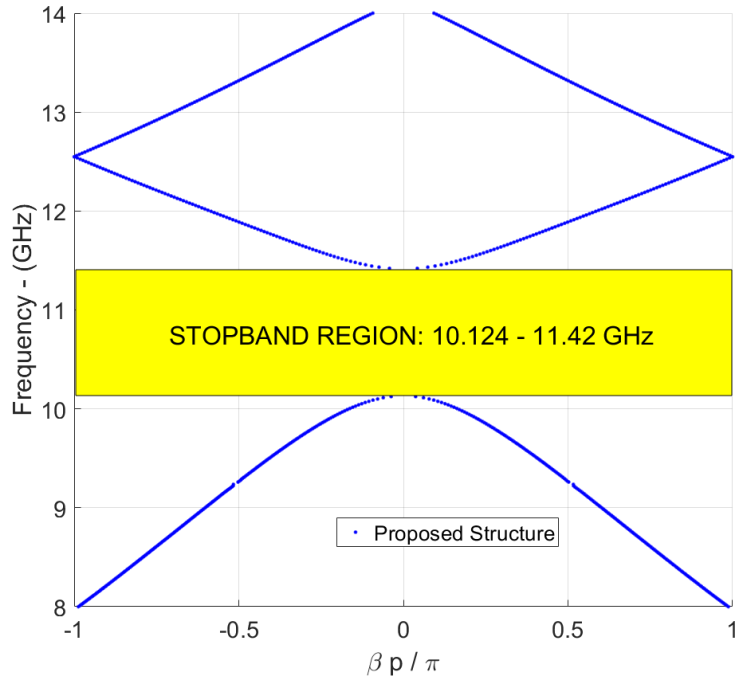

Figure 4. Dispersion diagram of proposed structure given in Figure 1 (c) with the following parameters: $C_1 = 14.8$mm, $C_2 = 0.7C_1$, $p_1 = 0.18541C_1$, $p_2 = 0.0925C_1$, $p_3 = 0.37C_1$, $h = 0.5$mm, $t = 0.035$mm, $\varepsilon_{r1} = 4.8$, $p = 2p_1 + 2p_2 + p_3 = 0.9245C_1$.

ended at 6.889 GHz, and the first stopband of this periodic structure occurs at 6.889-7.825 GHz, as shown in Figure 2. Unlike CS-1, CS-2 has a symmetric step discontinuity, starting from x = 0 and extending to (C1-C2) is formed in CS-2. The effect of this change on the dispersion diagram of the periodic structure is shown in Figure 3, where a wider stopband is slightly shifted to the upper frequency. Because of these modeling and simulations given in Figure 1(c), the dispersion diagram shown in Figure 4 can be obtained. Glide-symmetric modeling caused the stopband of the periodic structure to increase to higher frequencies and narrowed it with respect to CS-2. Figure 5 shows the electric and magnetic field distributions of two propagating Floquet modes obtained using the CST Eigenmode Solver. It is seen from Figure 5 that the first propagating mode is TE_{10} and the second mode is TE_{20} from the field patterns. In addition, it is observed in Figure 5 that in the electric and magnetic field distributions, one is mostly at maximum in the regions where the other is at minimum. In addition, changes in the cross-section of the unit cell change the cut-off frequencies of the propagating Floquet modes in the unit cell. In addition, the length of each waveguide region along the z-axis seen in Figure 5 is also very important in the formation of passband/stopband regions according to the guided wavelength of the waveguide in the relevant region [15, 16].

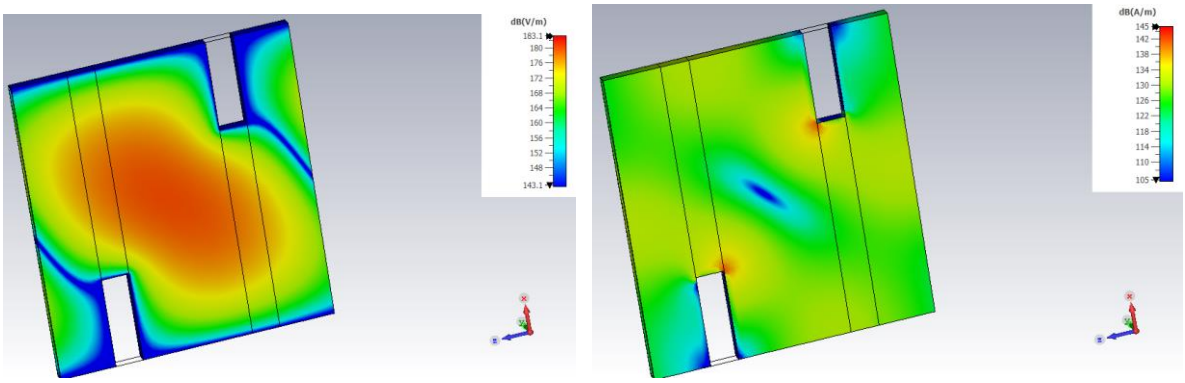

(a) E-field, The First Mode, 7.98GHz (b) H-field, The First Mode, 7.98GHz

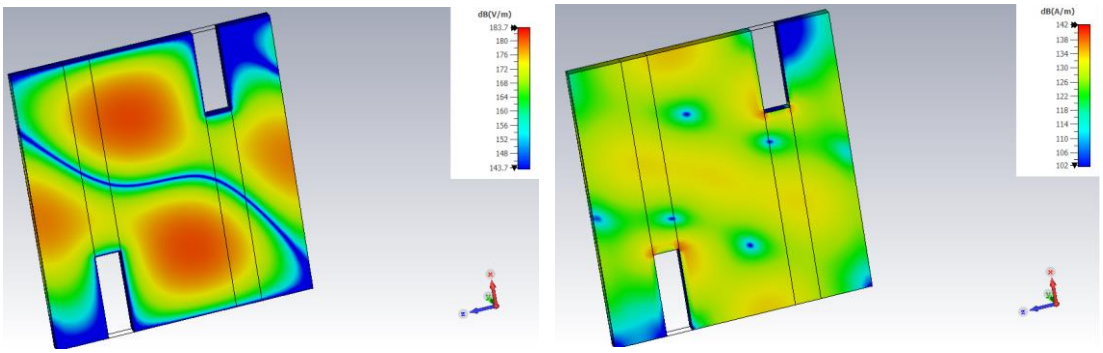

(c) E-field, The Second Mode, 12.55GHz (d) H-field, The Second Mode 1, 12.55GHz

Figure 5. Electric and magnetic field distributions of propagating Floquet modes for different frequencies.

3. Results and Discussions

In this section, the frequency characteristics of various numbers of cascade-connected unit cells, whose dispersion properties were determined in Section 2, will be analyzed.

3.1. Finite Modeling of Periodic Dielectric Loading of Rectangular Waveguides with glide symmetric step discontinuity

To observe the bandstop or bandpass filter characteristics, simulations of all the studied models with a finite number of periodic arrays are given in Figures 6-8. First, the frequency characteristics of the first mode of $|S_{21}|$ of the 10 waveguide modes were plotted for all models. As it is well known, it is expected that as the periodic sequence increases, a stopband region very close to the stop band obtained in the dispersion diagram of the periodic structure is formed. In addition, a deeper level of suppression appears as the number of unit cells increases. However, increasing the number of unit cells increased the ripple levels in the passband. Figure 6 shows $|S_{21}|$ frequency characteristics of CS-1 for N = 10, N = 15, and N = 20, where N is the number of unit cells.

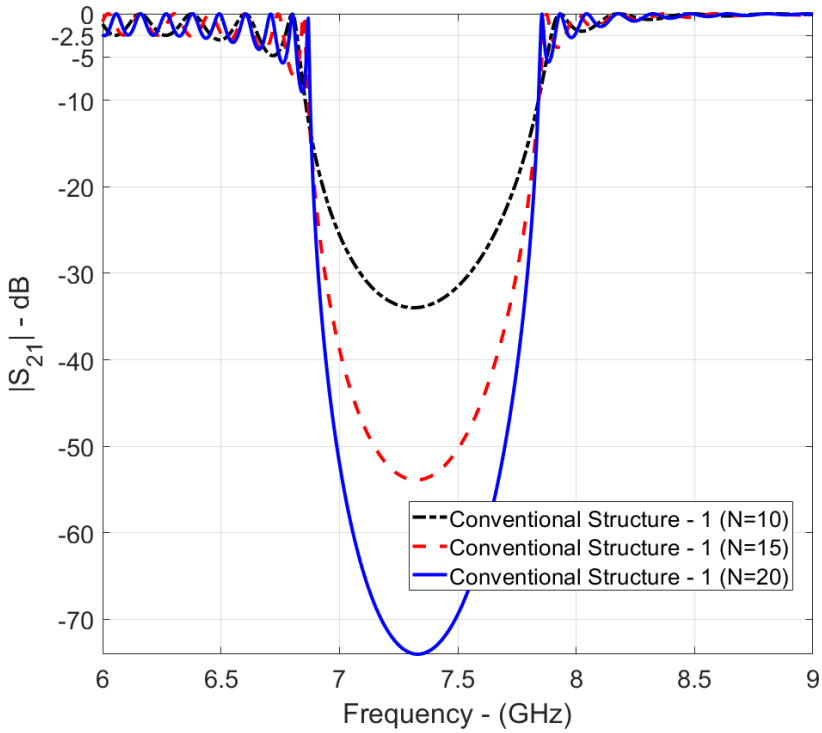

Figure 6. $|S_{21}|$ frequency characteristics of conventional structure - 1 given in Figure 1(a) with given parameters in Figure 2 for different cascaded scenarios.

Figures 7 and 8 show $|S_{21}|$ frequency characteristics of CS-2 and PS for N = 3, N = 5, N = 7, and N = 10, respectively. It can be clearly observed that the occurrence of symmetric step discontinuity (CS-2) leads to a wider and deeper stopband with fewer unit cells; however, this

leads to higher levels of fluctuations in the passband (close to -15dB). Switching from symmetric step discontinuity (CS-2) to glide symmetric step discontinuity (PS) with fewer unit cells results in a wider passband (7 – 10 GHz) and lower ripple levels (maximum -2.5 dB) in this passband, as shown in Figures 7 and 8. However, the stopband region has shifted, and the formation of a passband at higher frequencies is no longer valid. To compare the three models at the same dimensions, the number of unit cells was kept as high as possible to obtain a sufficiently deeper stopband.

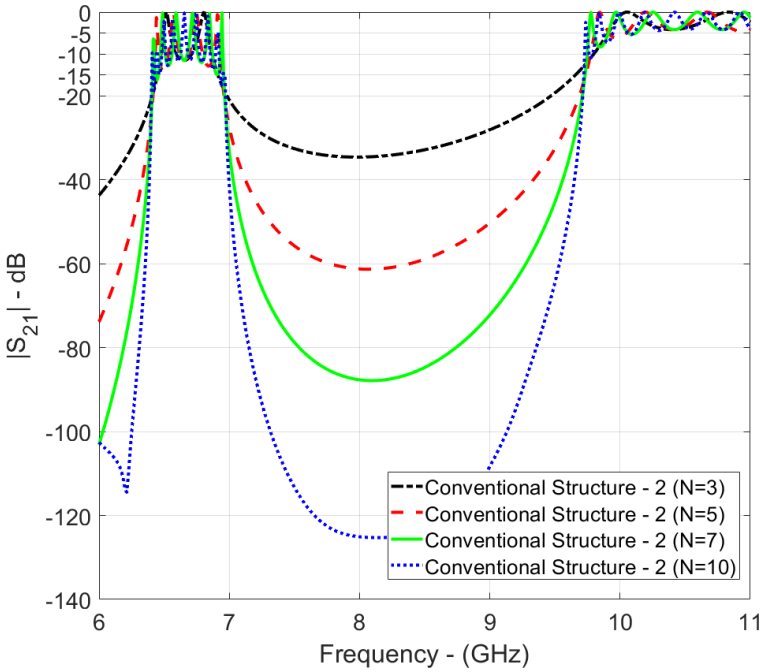

Figure 7. $|S_{21}|$ frequency characteristics of conventional structure - 2 given in Figure 1(b) with given parameters in Figure 3 for different cascaded scenarios.

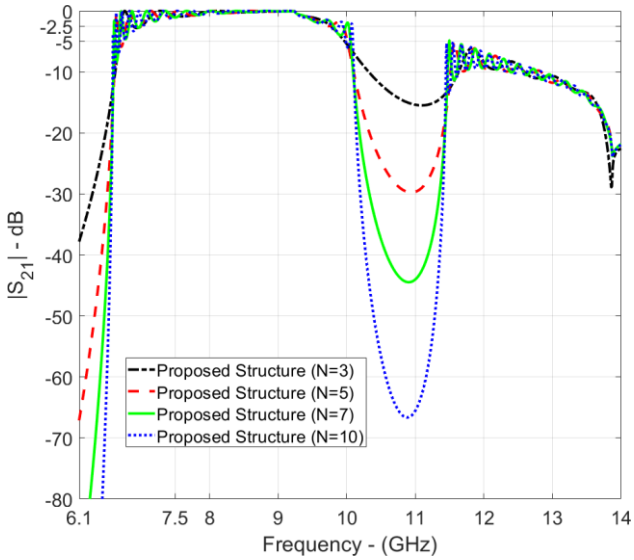

Figure 8. $|S_{21}|$ frequency characteristics and the proposed structure given in Figure 1(c) with given parameters in Figure 4 for different cascaded scenarios.

To compare and understand the frequency effects of different unit cell models called CS-1, CS-2, and PS, finite implementations of these structures for N=10 are carried out in CST Microwave Studio as shown in Figure 9. The parameter *t* is critical to understand the evaluation of the frequency response in the proposed structure. For this purpose, a parametric analysis showing the effect of the parameter t for N=10 is shown in Figure 10. In the curves ranging from *t*=0 to *t*=p/2, the passband in the range of 6.2 - 7.5 GHz and the fluctuations occurring there gradually decreased and reached very low levels. In addition, Figure 10 shows that in the

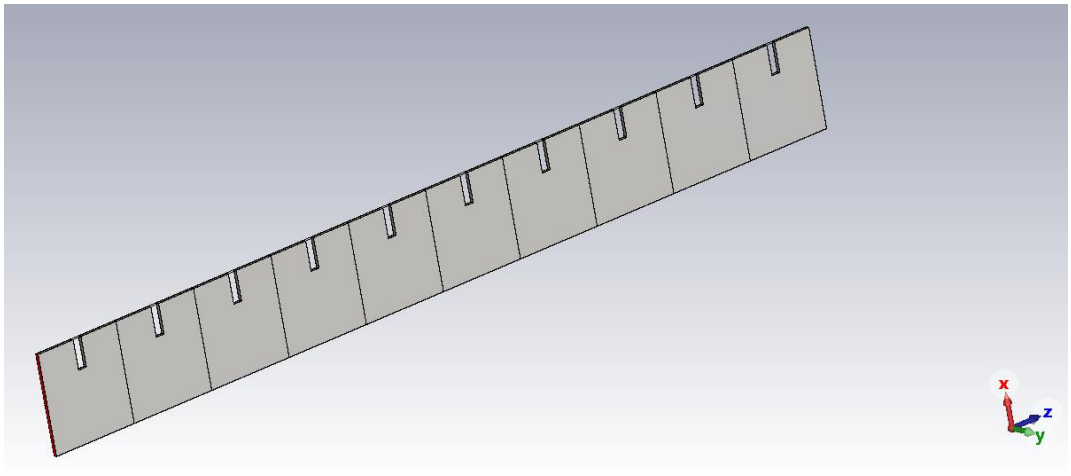

(a)

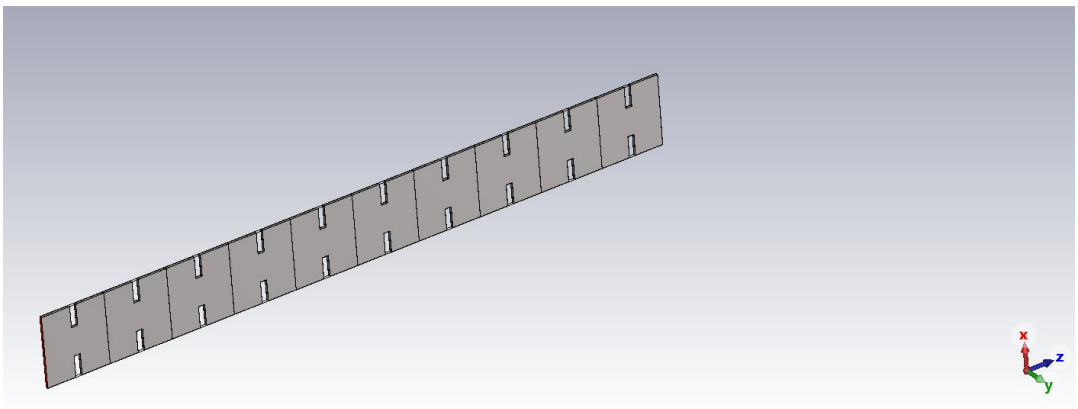

(b)

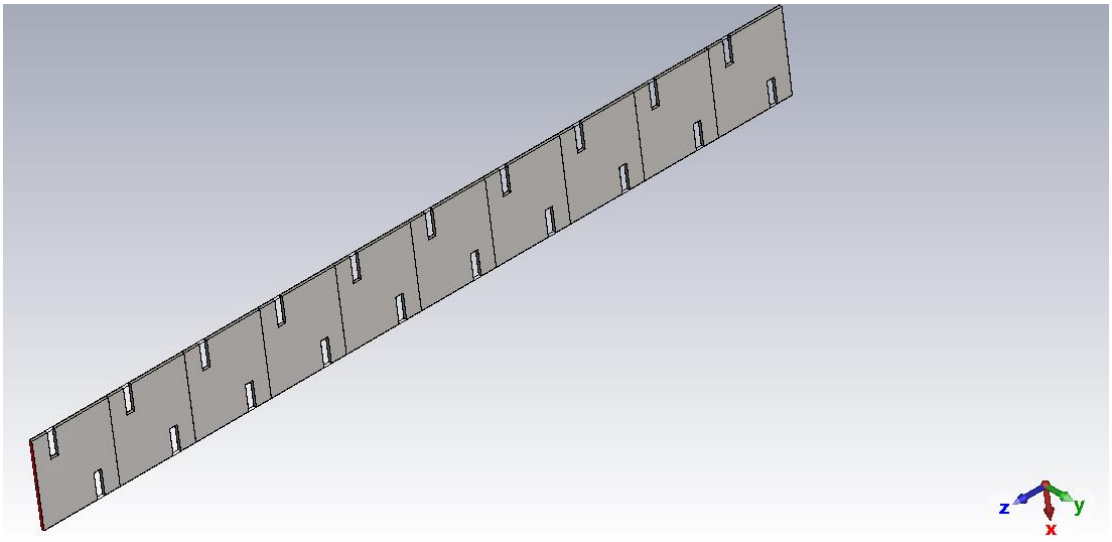

(c)

Figure 9. 3D view of cascaded-connected considered unit cells for N=10 in CST Microwave Studio.

same curves, the stopband between 7-9.8 GHz is replaced by a passband around 6.5-10 GHz. It is also possible to see in Figure 10 that the passband fluctuations gradually decrease at higher frequencies. It is clear from Figure 10 that this level of double step discontinuity given in this paper causes very high levels of fluctuations in the passband of the structure. In addition, gliding the one-step discontinuity region along the periodicity axis without changing the period of the unit cell reduces both the passband ripple levels. It also results in a wider passband and a shift of the stopband to higher frequencies.

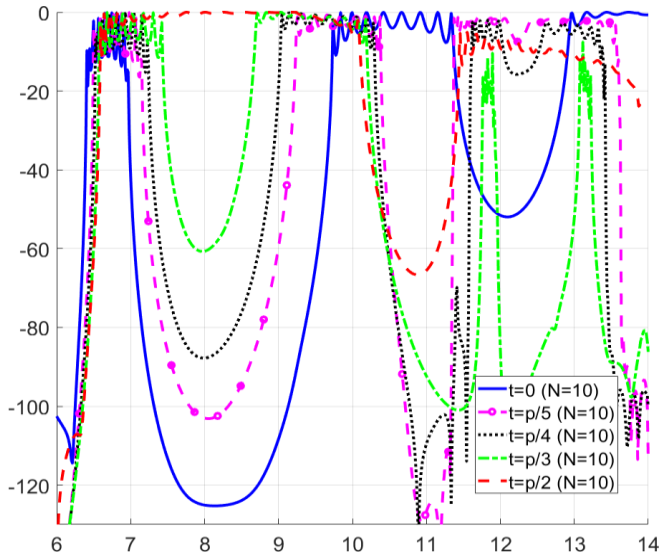

Figure 10. The effects of t parameters on the interested structure.

Accordingly, Figure 11 shows $|S_{21}|$ frequency characteristics of all three models for N = 10. According to Figure 11, the glide symmetric model allowed for a wider passband, as shown in Figure 11. In addition, the application of glide symmetry to the considered structure improved the fluctuation levels in the passband.

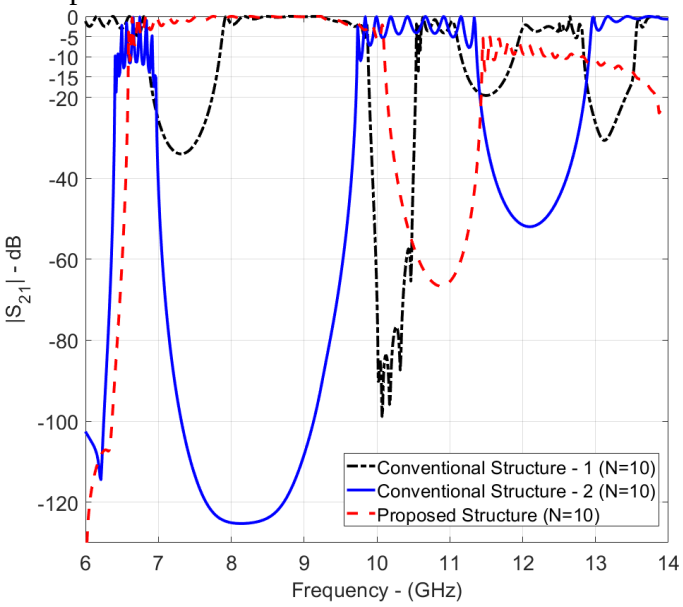

Figure 11. Comparison of $|S_{21}|$ frequency characteristics of given structures for N=10.

The frequency characteristics of the PS N=10 model were compared with those of similar designs in the literature, and the results are given in Table 1. According to the literature with very similar stopband characteristics, the best suppression level was obtained in the proposed study (PS, N=10). On the other hand, the proposed structure ranked second after [20] in terms of compactness in the compared studies.

Table 1. Comparison of the proposed structure with previous studies.

Studies	*Bandstop Region for -20 dB* $\|S_{21}\|$	*% FBW for* $-20\ dB$ *	*Suppression level min* S_{21} *(dB)*	*Circuit Size (mm × mm ×mm)*
[2], fig. 5	10-11.32	12.38	-48	10.16.× 22.86 × 301.84
[20], fig. 20	10.7-10.85	1.39	-30	10.16 ×22.86 × 16.957
PS N=10	10.14-11.429	11.95	-66	14.8×0.5× 136.826

*FBW can be calculated as follows: %FBW=$(f_2 - f_1)/f_0$ where $f_0 = (f_2 + f_1)/2$. f_0, f_1 and f_2 are center, lower and upper frequency of the stopband region with respect to -20 dB.

4. Conclusion

In this paper, a comparative analysis of a rectangular waveguide unit cell with homogeneous dielectric-loaded glide symmetric step discontinuity and conventional structures is presented, and its implications for filter design are investigated. The glide-symmetric unit cell structure produced a narrower stopband (between 10.124 and 11.42 GHz) than the other considered models. For N = 10, a wider passband with a lower ripple level (between 7-10 GHz and less than -2.5 dB) was obtained among all the modeled structures. The passband/stopband characteristics of the proposed structure demonstrate that these structures can be used in filter applications. Classical filter theory or direct coupling matrix synthesis approaches [21] can be used in each unit cell design of the proposed structure to minimize passband ripples and achieve the filter design goals. Higher-order symmetries can play an important role in achieving a wider passband. In this respect, different types of higher-order symmetries [12, 13] can be applied to rectangular waveguides with homogeneous dielectric-loaded step discontinuity in future studies.

Ethics in Publishing

There are no ethical issues regarding the publication of this study.

Author Contributions

Agah Oktay Ertay prepared organization and concept of the paper, wrote the whole paper; materials, methods, simulations, results and discussions and conclusions.

References

[1] Brillouin L., (1953) Wave Propagation in Periodic Structures, 2nd ed. New York: Dover.

[2] Şimşek, S., Topuz, E., Niver, E. (2012) A novel design method for electromagnetic bandgap based waveguide filters with periodic dielectric loading. AEU-International Journal of Electronics and Communications, 66(3), 228-234.

[3] Simsek, S., Topuz, E. (2007) Some properties of generalized scattering matrix representations for metallic waveguides with periodic dielectric loading. IEEE transactions on microwave theory and techniques, 11(55), 2336-2344.

[4] Coves, A., San-Blas, A. A., Bronchalo, E. (2021) Analysis of the dispersion characteristics in periodic Substrate Integrated Waveguides. AEU-International Journal of Electronics and Communications, 139, 153914.

[5] Mesa, F., Rodríguez-Berral, R., Medina, F. (2018) On the computation of the dispersion diagram of symmetric one-dimensionally periodic structures. Symmetry, 10(8), 307.

[6] Zuo, L., Wang, K., Li, Y., Liang, Z., Zheng, S. Y., Long, Y. (2020) The periodic leaky-wave antenna with different unit cells based on consistent fundamental mode. IEEE Transactions on Antennas and Propagation, 68(12), 7794-7802.

[7] Palomares-Caballero, Á., Alex-Amor, A., Padilla, P., Valenzuela-Valdés, J. F. (2020) Dispersion and filtering properties of rectangular waveguides loaded with holey structures. IEEE Transactions on Microwave Theory and Techniques, 68(12), 5132-5144.

[8] Valerio, G., Sipus, Z., Grbic, A., Quevedo-Teruel, O. (2017) Accurate equivalent-circuit descriptions of thin glide-symmetric corrugated metasurfaces. IEEE Transactions on Antennas and Propagation, 65(5), 2695-2700.

[9] Sipus, Z., Bosiljevac, M. (2019) Modeling of glide-symmetric dielectric structures. Symmetry, 11(6), 805.

[10] Tomić, D., Šipuš, Z. (2024) Rigorous Coupled Wave Analysis of Parallel-Plate Waveguides Loaded With Glide-Symmetric Dielectric Structures. Ieee Transactions on Microwave Theory and Techniques.

[11] Quevedo-Teruel, O., Chen, Q., Mesa, F., Fonseca, N. J., Valerio, G. (2021) On the benefits of glide symmetries for microwave devices. IEEE Journal of Microwaves, 1(1), 457-469.

[12] Quevedo-Teruel, O., Valerio, G., Sipus, Z., Rajo-Iglesias, E. (2020) Periodic structures with higher symmetries: their applications in electromagnetic devices. IEEE Microwave Magazine, 21(11), 36-49.

[13] Dahlberg, O., Mitchell-Thomas, R. C., Quevedo-Teruel, O. (2017) Reducing the dispersion of periodic structures with twist and polar glide symmetries. Scientific reports, 7(1), 10136.

[14] Fayzi, A., (2002) Dikdörtgen kesitli dalga kılavuzunda kesim ötesi değişikliklerin incelenmesi, İstanbul Teknik Üniversitesi Fen Bilimleri Enstitüsü, Yüksek Lisans Tezi.

[15] Berksoy, Z., (2013) SIW dalga kılavuzlarının analizi ve tasarım uygulamaları, İstanbul Teknik Üniversitesi Fen Bilimleri Enstitüsü, Yüksek Lisans Tezi.

[16] Bayraktar, F. A., (2013) Periyodik olarak yüklü dikdörtgen dalga kılavuzlarında bloch empedansı ve uygulamaları, İstanbul Teknik Üniversitesi Fen Bilimleri Enstitüsü, Yüksek Lisans Tezi.

[17] Hessel, A., Chen, M., Oliner, A. A. (1973) Propagation in periodically loaded waveguides with higher symmetries. Proceedings of the IEEE, 61(2), 183-195.

[18] Hamid, A. K. (1988) Moment method solution for multiple-step discontinuities in waveguides. University of Manitoba, Master thesis.

[19] Ertay, A. O., Şimşek, S. (2018). A comprehensive auxiliary functions of generalized scattering matrix (AFGSM) method to determine bandgap characteristics of periodic structures. AEU-International Journal of Electronics and Communications, 94, 139-144.

[20] Mrvić, M. V., Potrebić, M. M., Tošić, D. V. (2017) Compact h-plane dual-band bandstop waveguide filter. Journal of computational electronics, 16, 939-951.

[21] Cameron R. J., Kudsia C. M., Mansour R. R., (2018) Microwave filters for communication systems. Hoboken, NJ, USA: John Wiley &Sons, Ltd. Inc.